

This document is published at:

Mencía A., Chamorro C., Bonafont J., Duarte B., Holguin A., Illera N., Llamas, S.G., Escámez M.J., Hauser I., Del Río M., Larcher F., Murillas R. (2018). Deletion of a Pathogenic Mutation-Containing Exon of COL7A1 Allows Clonal Gene Editing Correction of RDEB Patient Epidermal Stem Cells. *Molecular Therapy Nucleic Acids*, 11, pp. 68-78.

DOI: <https://doi.org/10.1016/j.omtn.2018.01.009>



Funding entities: FEDER/Ministerio de Ciencia, Innovación y Universidades-Agencia Estatal de investigación SAF2017-86810-R y SAF2013-43475-R

© 2018 The Authors



This work is licensed under a Creative Commons Attribution-NonCommercial-NoDerivatives 4.0 International License.

Deletion of a Pathogenic Mutation-Containing Exon of *COL7A1* Allows Clonal Gene Editing Correction of RDEB Patient Epidermal Stem Cells

Ángeles Mencía,^{1,4,5,6} Cristina Chamorro,^{2,4,5,6} Jose Bonafont,^{2,4} Blanca Duarte,^{1,4,5} Almudena Holguin,^{1,4,5} Nuria Illera,^{1,4,5} Sara G. Llames,⁵ Maria José Escámez,^{2,4,5} Ingrid Hausser,³ Marcela Del Río,^{1,2,4,5} Fernando Larcher,^{1,2,4,5} and Rodolfo Murillas^{1,4,5}

¹Epithelial Biomedicine Division, Centro de Investigaciones Energéticas Medioambientales y Tecnológicas (CIEMAT), Madrid, Spain; ²Department of Biomedical Engineering, Carlos III University (UC3M), Madrid, Spain; ³Institute of Pathology, Universitätsklinikum Heidelberg, Heidelberg, Germany; ⁴Instituto de Investigación Sanitaria de la Fundación Jiménez Díaz, Madrid, Spain; ⁵Centro de Investigación Biomédica en Red en Enfermedades Raras (CIBERER) U714, Madrid, Spain

Recessive dystrophic epidermolysis bullosa is a severe skin fragility disease caused by loss of functional type VII collagen at the dermal-epidermal junction. A frameshift mutation in exon 80 of *COL7A1* gene, c.6527insC, is highly prevalent in the Spanish patient population. We have implemented gene-editing strategies for *COL7A1* frame restoration by NHEJ-induced indels in epidermal stem cells from patients carrying this mutation. TALEN nucleases designed to cut within the *COL7A1* exon 80 sequence were delivered to primary patient keratinocyte cultures by non-integrating viral vectors. After genotyping a large collection of vector-transduced patient keratinocyte clones with high proliferative potential, we identified a significant percentage of clones with *COL7A1* reading frame recovery and Collagen VII protein expression. Skin equivalents generated with cells from a clone lacking exon 80 entirely were able to regenerate phenotypically normal human skin upon their grafting onto immunodeficient mice. These patient-derived human skin grafts showed Collagen VII deposition at the basement membrane zone, formation of anchoring fibrils, and structural integrity when analyzed 12 weeks after grafting. Our data provide a proof-of-principle for recessive dystrophic epidermolysis bullosa treatment through *ex vivo* gene editing based on removal of pathogenic mutation-containing, functionally expendable *COL7A1* exons in patient epidermal stem cells.

INTRODUCTION

Recessive dystrophic epidermolysis bullosa (RDEB) is a severe skin fragility disease caused by loss-of-function mutations in *COL7A1*, a gene expressed by keratinocytes and fibroblasts that encodes type VII collagen (C7), the main constituent of the anchoring fibrils necessary for adhesive connection between the dermis and the epidermal basement membrane zone (BMZ). C7 deficiency results in severe and recurrent blistering of the skin and other stratified epithelia, scarring, and highly increased risk for development of metastatic squamous cell carcinoma.¹ *Ex vivo* gene therapy strategies for epidermolysis bullosa, including junctional epidermolysis bullosa

and RDEB, based on transplantation of retroviral vector-modified keratinocyte sheets are already in a clinical stage with promising results.^{2–5} Also, an approach using graftable bioengineered skin equivalents containing RDEB fibroblasts and keratinocytes corrected by means of a SIN-retroviral vector will soon be tested in patients.⁶ However, although gene addition tackles the wide range of disease-causing mutations, retroviral vector-based gene transfer poses biosafety concerns including inaccurate spatial-temporal gene expression and potential genotoxicity risks. Moreover, the efficacy of retroviral vectors for the long-term correction of autologous skin grafts is not clearly established yet.⁴ Thus, gene therapy protocols for monogenic disease correction are moving from retroviral vector-based gene replacement to more precise gene-editing approaches for highly specific interventions on the defective gene at DNA and RNA levels.

Experimental demonstrations of gene-editing approaches for RDEB therapy have included protocols based on patient-derived induced pluripotent stem cells (iPSCs)^{7–9} and direct correction of patient keratinocytes *ex vivo* by homology-directed repair (HDR)^{10–12} and non-homologous end joining (NHEJ) strategies.¹¹ “Skipping” of pathogenic mutation-containing exons has been proven an efficient strategy for the correction of hereditary diseases caused by mutations in genes coding for proteins with long, repetitive structural domains. The best-characterized case and proof of principle for exon-skipping therapy is dystrophin gene reading frame recovery by modulation of its pre-mRNA splicing with synthetic antisense oligonucleotides

Received 22 December 2017; accepted 23 January 2018;
<https://doi.org/10.1016/j.omtn.2018.01.009>

⁶These authors contributed equally to this work.

Correspondence: Rodolfo Murillas, PhD, Epithelial Biomedicine Division, Cutaneous Disease Modeling Unit, CIEMAT-CIBERER (Centre for Biomedical Research on Rare Diseases) U714, Avenida Complutense 40, Madrid 28040, Spain. E-mail: rodolfo.murillas@ciemat.es

Correspondence: Fernando Larcher, PhD, Epithelial Biomedicine Division, Cutaneous Disease Modeling Unit, CIEMAT-CIBERER (Centre for Biomedical Research on Rare Diseases) U714, Avenida Complutense 40, Madrid 28040, Spain. E-mail: fernando.larcher@ciemat.es



(AON) in Duchenne muscular dystrophy (DMD) muscle cells. Truncated dystrophin proteins lacking the sequence encoded by the skipped mutation-containing exons are partially functional, thus having the potential to shift the phenotype from severe to mild.¹³ A similar AON-based exon-skipping approach has been recently described for recessive RDEB.^{14–17} *COL7A1* is especially amenable to exon-skipping correction strategies since all exons encoding the triple-helix forming region, essential for the structural function of C7, are small, in frame, and encode Gly-X-Y repeats. The functionality of internally deleted Collagen VII variants lacking sequences encoded by specific collagenous domain exons has been demonstrated.^{15,17} However, despite advances to increase their stability and the feasibility of *in vivo* applications, AONs can only promote transient masking of splicing motifs and therefore allow for temporary correction of the genetic defect. Permanent exon-skipping-mediated gene repair can be achieved by introducing changes in the DNA sequence to eliminate intron-splicing motifs or exonic sequences all together. Highly specific programmable nucleases are able to generate DNA double-strand breaks in the proximity of the pathogenic mutation sequence that are resolved by the NHEJ DNA repair system, frequently leading to the introduction of insertion and deletion (indel) mutations. This NHEJ-mediated strategy was originally implemented for the *ex vivo* correction of DMD patient muscular cells^{18,19} and later demonstrated by our laboratory for the successful correction of RDEB patient-derived keratinocytes.¹¹ It has also proved feasible for the *in vivo* correction of DMD^{20–22} and RDEB in experimental mouse models when CRISPR/Cas9 were delivered by AAV vectors or as RNP particles.²³

Stringent biosafety standards, a necessary requirement for the implementation of gene therapy protocols, can be conceived by performing accurate genotyping and genomic characterization of gene-modified single epidermal stem cell clones with the potential to regenerate gene-corrected skin.^{24–26} The feasibility of clonal-based therapy with gene-targeted epidermal stem cells has been previously established by our laboratory with the demonstration that long-term skin regeneration from a human epidermal stem cell clone carrying a targeted integration of a marker gene at the AAVS1 locus can be attained.^{25,26} However, although studies in immortalized RDEB keratinocytes showed the feasibility of the approach,^{11,12} clonal therapy for RDEB based on isolation of epidermal stem cells modified by gene-editing protocols to re-establish production of functional C7 has not yet been achieved.

With the aim of developing a gene-editing-based therapy specifically tailored to the c.6527insC mutation in exon 80 of the *COL7A1* gene,²⁷ highly prevalent in the Spanish RDEB patient population,²⁸ we have previously delivered TALEN nucleases by adenoviral vectors able to introduce small deletions in the exon 80 of *COL7A1* gene that resulted in exon 80 skipping.¹¹ Using these tools, and after thorough analysis of a large collection of RDEB patient keratinocyte clones, we have now achieved long-term skin regeneration from several NHEJ-mediated *COL7A1* gene frame-restored clones, including a single epidermal stem cell clone with permanent exon deletion-based RDEB correction.

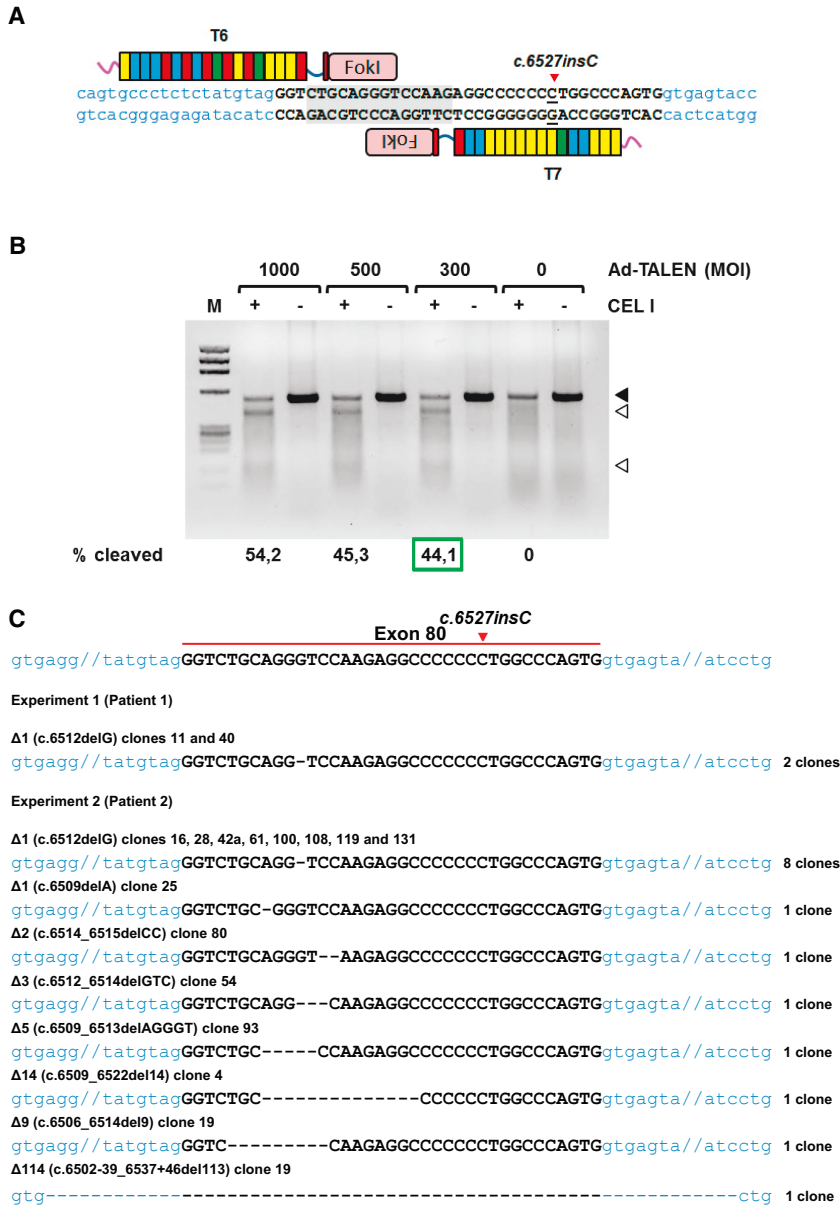
RESULTS

Transduction of Primary RDEB Keratinocytes with Ad-Talens and Isolation and Genotyping of Keratinocyte Clones Carrying Corrective Indels in *COL7A1* Exon 80

Primary keratinocytes from RDEB patients previously characterized as homozygous carriers for the highly prevalent c.6527insC *COL7A1* mutation²⁸ were infected with adenoviral vectors for the expression of TALEN nucleases T6/T7,¹¹ specific for *COL7A1* exon 80 (Figure 1A). Different MOIs were assessed to establish the optimal conditions for indel generation in primary RDEB keratinocytes, as determined by Cel I analysis. A MOI of 300 was the lowest to yield high indel generation (Figure 1B) without noticeable reduction in cell viability. Cells from two different patients (P1 and P2) infected at optimized conditions, were split at low density to isolate individual clones. Genotyping of clones was performed by sequencing a PCR amplicon spanning the nuclease target site. In the first experiment using cells from P1, 22 keratinocyte clones were isolated and genotyped, two of which (clones 11 and 40) carried a 1-nucleotide (guanine) deletion allele, c.6512delG (named as ΔG) at the TALENs target site, corresponding to the most frequent deletion detected in our previous editing experiments with immortalized RDEB keratinocytes¹¹ using the same TALEN nucleases pair (experiment 1, Figure 1C). The other 20 clones in this experiment were unmodified, presenting the c.6527insC allele sequence. Previously, we showed that the ΔG deletion resulted in a frameshift leading to frame restoration in c.6527insC *COL7A1* mutation-bearing RDEB keratinocytes, causing the expression of a variant transcript encoding a four-amino-acid substitution in C7.¹¹ Transcripts encoding this C7 variant were also found in P1 clones 11 and 40 when *COL7A1* expression was analyzed by sequencing RT-PCR products spanning exons 78 to 84 (Figures S1A and S1B).

When the experiment was repeated using cells from P2, a larger collection of keratinocyte clones were isolated and expanded, which allowed us to screen a broader spectrum of indels. In this experiment, 14 out of 125 clones analyzed carried indels and the ΔG 1-bp deletion was again the most commonly found (eight clones). In addition, one clone with a different frame-restoring 1-bp deletion, four clones carrying non-correcting mutations, and one clone (clone 19) with a 114-bp deletion entirely encompassing exon 80 were identified (experiment 2, Figure 1C). All the other clones were unmodified c.6527insC homozygous carriers.

Analysis of the sequence chromatograms of PCR products spanning the TALEN target site revealed that clone 11 carried one ΔG deletion allele, while clone 40 was biallelically modified for this mutation (Figure 2A). A careful analysis of the chromatogram for clone 19 revealed multiple overlapping traces corresponding to different *COL7A1* alleles. Therefore, the PCR product for clone 19 was TA-cloned, and individual colonies were sequenced, revealing the presence of three alleles: c.6527insC (pathogenic mutation, unedited), c.6502-39_6537+46del113 (114-bp deletion, encompassing exon 80 entirely), and c.6503_6511del9 (9-bp deletion) (Figure 2B).



The 9-bp deletion found in the c.6503_6511del9 allele was within the exon 80 sequence and not consistent with *COL7A1* frame restoration. Immunofluorescence analysis of ΔG deletion-carrying clones 11 and 40 using an anti-human C7 monospecific polyclonal antibody¹⁷ showed strong and homogeneous C7 staining (Figure 2C, upper panels). In contrast, and consistent with the presence of three different *COL7A1* alleles, immunofluorescence analysis of clone 19 revealed the presence of C7-positive and -negative cells (Figure 2C, lower right panel) in similar proportions, indicating that this clone may be comprised of a bi-clonal population. A clone from experiment 2 that did not contain any indels (clone 31) was used as a negative staining control (Figure 2C, lower left panel).

Figure 1. Indel Generation with TALEN Nucleases in Primary RDEB Patient Keratinocytes

(A) TALEN pair T6/T7 targets the 5' region of the *COL7A1* exon 80 sequence (upper case) in the vicinity of the c.6527insC mutation (red arrowhead). TALEN spacer sequence is shaded. Intron sequences are in blue lower case. (B) The PCR product comprising the T6/T7 target site was analyzed with Surveyor (Cel I) mutation detection assay to establish optimal MOI in patient keratinocytes infected with adenoviral vectors for T6/T7 TALEN expression. Solid arrowhead indicates uncleaved DNA; arrowheads indicate cleavage fragments. Percentage of cleavage for each PCR product is shown at the bottom. M is IX molecular weight marker. (C) Indel spectrum in keratinocytes from RDEB patients 1 (experiment 1) and 2 (experiment 2) transduced with Ad-T6/T7 vectors. Two out of 22 clones in experiment 1 and 14 out of 125 clones in experiment 2 carried indel alleles at the TALEN target site. The number of clones containing each indel is shown on the right. Intron sequences are in blue lowercase letters. Double slash marks represent DNA sequences that are not shown.

Isolation and Characterization of Pure Clones from Clone 19 Mixed Population

To isolate pure keratinocyte clones carrying the exon 80-excising 114-bp deletion allele, limiting dilution subculture of the clone 19 mixed population was performed. C7 immunofluorescence analysis showed that, in contrast to the mixed C7-positive and -negative pattern found in parental clone 19 mixed population, all cells in each keratinocyte subclone were either completely positive or negative for C7 staining. Two C7-expressing clones with proliferative potential, named as 19.3 and 19.C, and one C7-negative clone, named as 19n, were expanded for further experimentation (Figure 3A). PCR analysis with primers spanning the 114-bp deletion revealed that, for clones 19.3 and 19.C, the higher and lower molecular weight bands, whose mobility corresponds to the undelated (Figure 3A, black arrowhead) and deleted (Figure 3A, red arrowhead) alleles, respectively, were of comparable intensity, unlike in the parental clone 19. For the C7-negative clone 19n, only the higher-molecular-weight band was detected (Figure 3B). The intermediate molecular weight band detected in all C7-expressing clones (19, 19.3, and 19.C) most likely corresponds to heteroduplex DNA formation between deleted and undelated alleles, as previously reported for PCR genotyping of cells carrying deletion alleles in other genes.^{29,30} Furthermore, the Sanger sequencing chromatogram of PCR products for clones 19.3 and 19.C showed overlapping traces corresponding exclusively to c.6527insC (unmodified) and c.6502-39_c.6537+46del113 (114-bp deletion, ΔE80) alleles. These PCR products were cloned in a plasmid vector, and individual colonies were sequenced to unequivocally verify the presence of both alleles

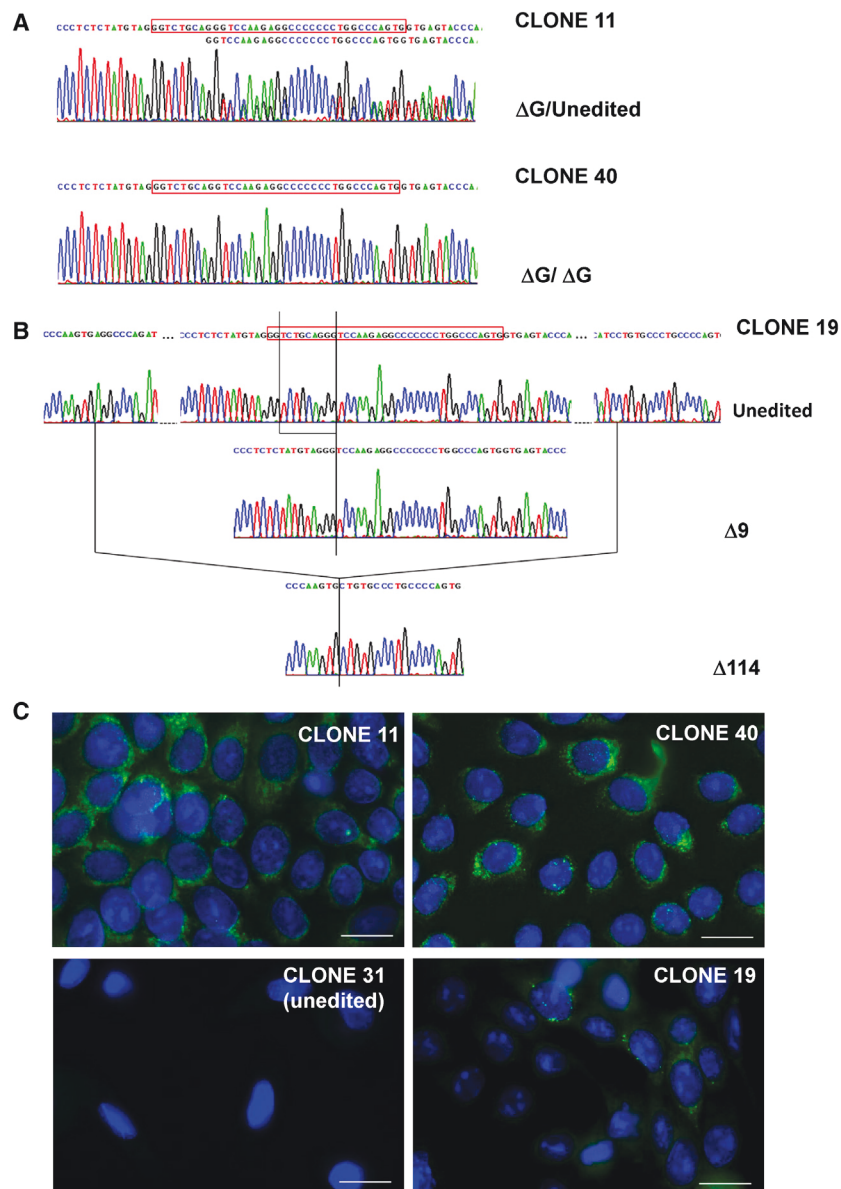


Figure 2. Genotypes of RDEB Patient Keratinocyte Clones Carrying Different Frame-Restoring Indels and Collagen VII Expression Analysis

(A) Sanger sequencing chromatograms of PCR products spanning the TALEN target site show the 1-bp ΔG deletion in one *COL7A1* allele (clone 11, upper chromatogram) or in both (clone 40, lower chromatogram). The exon 80 sequence is shown in the red box. (B) Chromatograms corresponding to individual colonies of the TA-cloned PCR product for clone 19 showed three different alleles: unedited (upper), 9-bp deletion ($\Delta 9$, middle), and 114-bp deletion ($\Delta 114$, lower). (C) Immunofluorescence staining with anti-C7 antibody showed C7 expression in approximately half of the cells in clone 19 and in all cells from clones 11 and 40.

these putative off-target cleavage sites, amplified from genomic DNA of clones containing the 114-bp exon 80 deletion (19, 19.3, and 19.C). Thirteen of the highest scoring off-target sites, located in loci different to *COL7A1* gene were analyzed. In addition, seven lower-scoring sites located within the *COL7A1* gene were scrutinized (Table S1) because of the potential detrimental effect of mutations introduced at these sites on our gene repair strategy. No nuclease off-target cleavage activity was detected in this analysis (Figure S3).

Since the 114-bp deletion completely eliminates the exon 80 of *COL7A1* gene, expression analyses were performed in mixed clone 19 and subclones 19.3 and 19.C to study the presence of gene transcripts lacking the exon 80-encoded sequence and therefore with restored open reading frame. RT-PCR analysis of RNA samples from clones 19, 19.3, and 19.C produced bands with a molecular weight corresponding to the unedited (Figure 4A, black arrowhead) and exon 80-deleted (red arrowhead) alleles. In pure clones, 19.3, and 19.C, the smaller molecular weight band corresponding to a shortened, frame-restored transcript lacking the exon

(Figure 3C). The c.6503_6511del9 (9-bp deletion) allele was not found in these clones, showing that this allele was present in the cellular subpopulation that was segregated from clones 19.3 and 19.C by subcloning. Consistently, genotyping of C7-negative clone 19n revealed the presence of overlapping chromatograms for the c.6527insC (unmodified) and c.6503_6511del9 (9-bp deletion) alleles in these cells (Figure S2).

To assess the specificity of TALENs activity, we identified genomic sites with the potential for off-target cleavage by using the PROGNOS software that ranks sites according to number of mismatches relative to the intended target sequence and repeat variable diresidue (RVD)-nucleotide binding frequencies.³¹ The presence of indel mutations was assessed by performing Cel I analysis of PCR products containing

80 sequence was more intense than the higher molecular weight band corresponding to the out-of-frame transcript generated from the unedited allele, which might be due to increased stability of the exon 80-deleted transcript. To verify that the 114-bp deletion resulted in splicing of *COL7A1* pre-mRNA such that exons 79 and 81 are joined together, the PCR products were TA-cloned and sequenced, revealing transcripts lacking the exon 80-encoded sequence (Figure 4B) in clones 19, 19.3, and 19.C. Transcripts containing the c.6527insC mutation encoded in the unedited allele were also found for all three clones. In addition, transcripts originating from the 9-bp deletion allele, which was not conducive to frame restoration, were found in mixed clone 19, but not in 19.3 and 19.C clones. To quantify the expression of edited and unedited alleles in these clones, quantitative real-time qPCR was performed using two probes, one

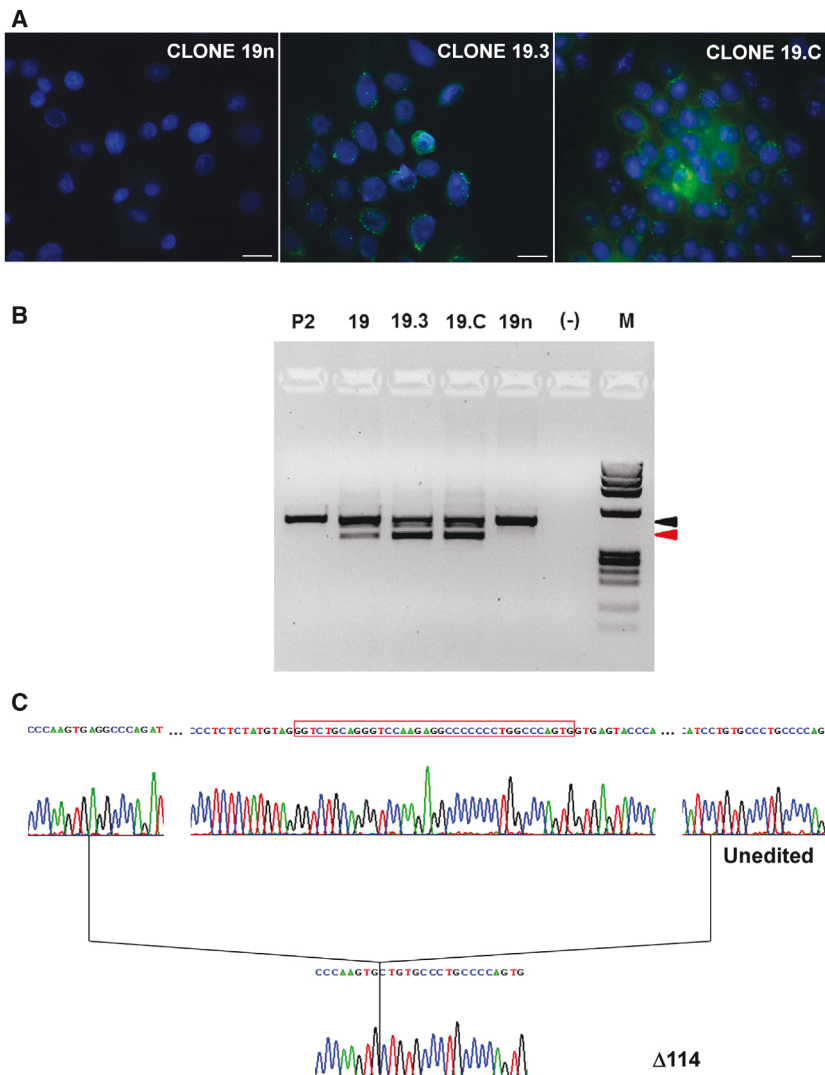


Figure 3. Isolation and Characterization of Pure Clones from Clone 19 Mixed Population

(A) C7 immunofluorescence analysis of subclones 19n, 19.3, and 19.C obtained by limiting dilution subculture of clone 19 mixed population. Scale bar, 20 μm . (B) PCR analysis for the detection of the 114-bp deletion in clone 19 and corresponding subclones 19.3, 19.C, and 19n. Undeleted (black arrowhead) and deleted (red arrowhead) alleles could be detected using primers spanning the deletion region. P2 genomic DNA from patient 2 keratinocytes was used as a control for amplification of the unedited allele. (-), negative control without DNA; M, IX molecular weight marker. (C) Sanger sequencing of TA-cloned PCR products demonstrated the presence of exclusively the unedited (upper chromatogram) and 114-bp deletion ($\Delta 114$, lower chromatogram) alleles in clones 19.3 and 19.C. Exon 80 sequence shown in red box. Black lines depict deletion boundaries.

frame restoration but causes a predicted four-amino-acid change (i.e., Gly-Pro-Arg-Gly to Val-Gln-Glu-Ala), disrupting the Gly-X-Y pattern characteristic of the triple helix forming domain.¹¹ Similarly, increased amounts of C7, compared to normal human keratinocytes, were found in clones 11 (monoallelic for ΔG deletion) and 40 (biallelic for ΔG deletion), isolated in the experiment with patient P1 cells, by western blot (Figure S1C). Increased C7 might be explained by intracellular retention of the protein due to hindered secretion caused by defective triple-helix formation.

In Vivo Skin Regeneration with Frame-Restored Clones: C7 Deposition and Functional Analysis

To evaluate the functional effect of C7 expression recovery either by *COL7A1* frame restoration by a 1-bp deletion that resulted in a four-amino-acid substitution (clones 11 and 40) (Figure 5A) or

recognizing the *COL7A1* exon 64 sequence (probe Ex64) and therefore detecting transcripts produced by both the edited and unedited alleles and other recognizing the exon 80 sequence that will detect only transcription from the unedited, exon 80 sequence-containing allele (probe Ex80). For all three clones, *COL7A1* expression was higher with Ex64 probe than with Ex80 probe, proving that most of *COL7A1* transcription in these gene-edited clones originates from the edited allele lacking the exon 80 sequence (Figure 4C).

C7 protein expression in keratinocyte clones was analyzed by western blotting (WB) using an anti-human C7 monospecific polyclonal antibody.¹⁷ The amount of C7 in gene-edited clones was comparable to that found in an unaffected patient sibling heterozygous for the null mutation (P2s) and somewhat lower than in normal human keratinocytes (Figure 4D). Interestingly, higher C7 expression was found in gene-edited clone 61, isolated in the experiment with patient P2 cells and carrying the ΔG , 1-bp deletion allele that results in *COL7A1*

exon 80 deletion (clones 19 and 19.C) (Figure 6A), skin equivalents prepared with keratinocytes from the different clones, and C7 null fibroblasts were grafted onto immunodeficient mice. The dermal-epidermal adhesion phenotype and C7 deposition at the BMZ was analyzed 12 weeks after grafting, a time point indicative of long-term skin regeneration. Skin engraftment occurred for the four clones and, macroscopically, the regenerated skin appeared normal (Figures 5B, 5C, and 6B). However, grafts from clones 11 and 40 showed marked fragility as epidermis was easily separated from the dermis upon mild pulling from the edge of an incision performed on the engrafted human skin using a scalpel (Figures 5D–5E; Figure S4). On the contrary, skin regenerated from both mixed clone 19 and clone 19.C showed mechanical resistance to the pulling test (Figure 6C). Immunofluorescence analysis clearly showed C7 expression in grafts from all clones. Interestingly, in grafts from clones 11 (Figure 5F) and 40 (Figure 5G), C7 was not at the BMZ, the physiological location of this protein in skin grafts from normal human keratinocytes

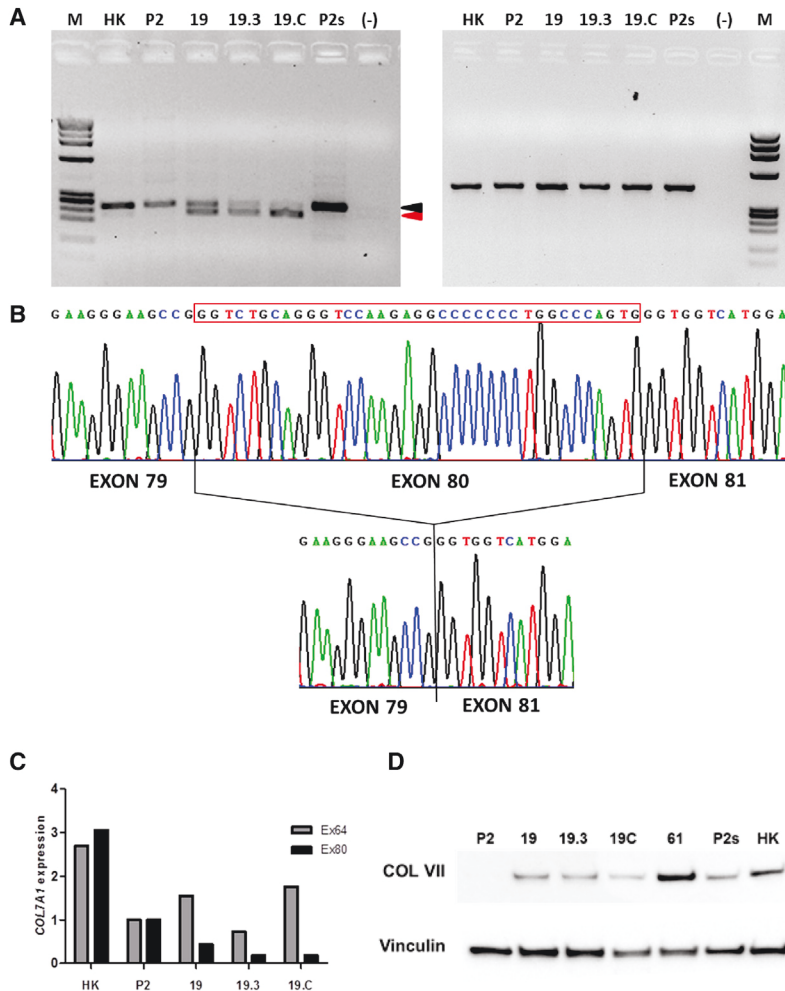


Figure 4. COL7A1 Gene Expression Analysis in Frame-Restored Clones

(A) RT-PCR analysis for detection of *COL7A1* transcripts using primers in exons 78 to 84. A 240/241-bp band (black arrowhead) corresponding to wild-type/c.6527insC unedited transcripts was amplified from all RNA samples (left). In addition, a 205-bp band (red arrowhead) corresponding to exon 80-lacking transcripts was found in clones 19, 19.3, and 19.C. M, IX molecular weight marker; HK, healthy human keratinocytes; P2, patient keratinocytes; P2s, healthy heterozygous patient sibling; (-), negative control without cDNA. GAPDH expression was analyzed as a loading control (right). (B) TA-cloned RT-PCR products from clones 19, 19.3, and 19.C revealed the presence of transcripts originating from the unedited pathogenic allele (upper chromatogram) and transcripts lacking the exon 80-encoded sequence (lower chromatogram). Black lines depict exon boundaries. Chromatograms corresponding to clone 19.C are shown. (C) Real-time qPCR quantification of *COL7A1* expression using Taqman probes specific for all *COL7A1* transcripts (Ex64) and exon 80-containing transcripts (Ex80). (D) Western blot analysis of C7 expression. P2, patient 2 keratinocytes; 19, 19.3, 19.C, clones from P2 carrying the 114-bp deletion allele; 61, clone from P2 carrying the Δ G 1-bp deletion allele; P2s, healthy heterozygous sibling keratinocytes; HK, healthy human keratinocytes.

arrowheads), demonstrating that not only is the C7 protein lacking exon 80-encoded sequence properly produced and secreted but it is also fit for anchoring fibril formation.

DISCUSSION

To achieve the generation of persistent genetically corrected skin grafts with therapeutic potential, targeting epidermal stem cells is necessary. Our laboratory first demonstrated the feasibility of

(Figure 5H), but it was instead retained within the cytoplasm of basal keratinocytes, indicating a faulty secretion of the C7 variant produced by these cells. In contrast, grafts from clones 19 and 19.C, showed correct C7 deposition at the BMZ zone (Figure 6F) with the same pattern as in grafts generated from normal human keratinocytes (Figure 6G). No C7 staining was found in grafts from unedited patient keratinocytes used as negative controls (Figures 5I and 6H). Blistering was evident in grafts from clones 11 and 40 and in the control graft from unedited patient keratinocytes (Figure 5F, 5G and 5I, asterisks). Grafts generated from the mixed clone 19 showed the presence of C7 negative patches likely corresponding to the cells carrying the non-correcting 9-bp deletion and matching blistering foci (Figure S5).

Epidermal-dermal adhesion and normal epidermal architecture of human skin grafts generated with gene-corrected patient keratinocytes from clone 19.C was verified by histological analysis (Figure 6D). Immunohistochemical staining using an antibody specific for human involucrin showed normal human epidermal differentiation in the skin graft (Figure 6E). Furthermore, ultrastructural analysis of grafts from clone 19.C showed the presence of mature anchoring fibrils (Figure 6I,

long-term skin regeneration from a single gene-targeted epidermal stem cell clone.²⁵ Here, we have achieved the *ex vivo* correction of a genodermatosis by gene editing in patient epidermal stem cells. Previous experimental approaches by our laboratory¹¹ and others^{7,10,12} had delineated protocols for recovery of C7 production in RDEB patient-derived keratinocytes using gene editing strategies. However, since studies based on selection of corrected clones have been performed either on immortalized keratinocyte cell lines,^{11,12} patient-derived iPSC lines⁷ or polyclonal populations without proven regenerative potential,¹⁰ they are still far from having clinical relevance. Moreover, most reported studies have relied on the use of drug selection to achieve correction by still highly inefficient HDR-based protocols.¹² We recently established drug-selection-free, NHEJ-based exon skipping strategies for highly efficient recovery of C7 expression in RDEB-derived keratinocytes.¹¹ Building upon this foundation, we have generated human skin from a single RDEB patient epidermal stem cell with normal dermal-epidermal adhesion features after recovering the expression of a functional C7 protein variant, lacking the exon 80-encoded fragment, from the endogenous mutant *COL7A1* gene. Although this protocol has

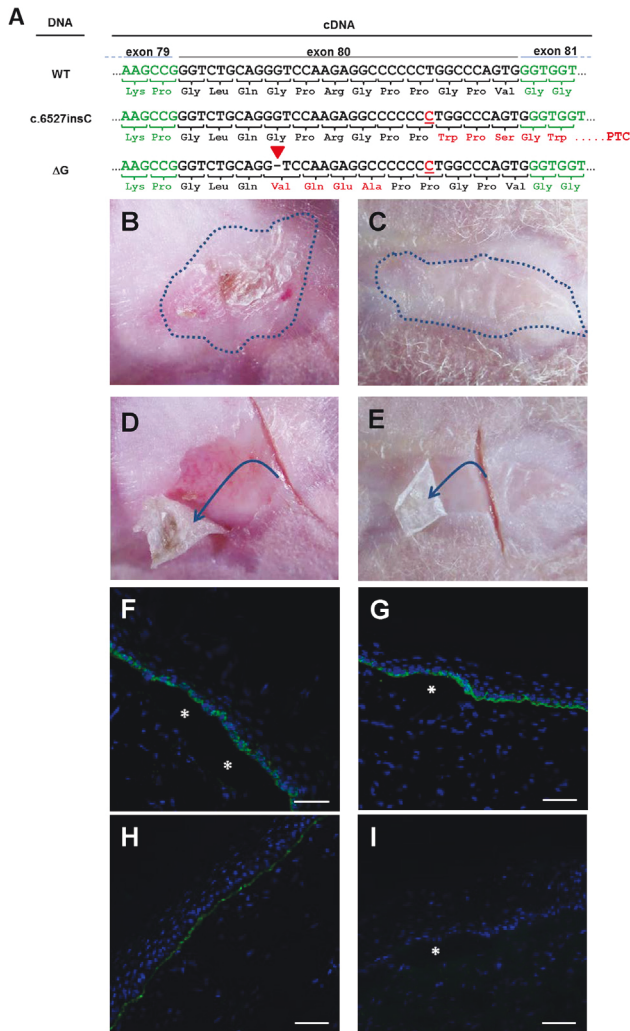


Figure 5. In Vivo Skin Regeneration from Frame-Restored Patient Keratinocyte Clones 11 and 40 Expressing a C7 Variant with a Four-Amino-Acid Substitution

(A) *COL7A1* cDNA and C7 amino acid sequences for WT, c.6527insC (cytosine insertion underlined in red), and Δ G (1-bp deletion, red arrowhead) alleles. Amino acid substitutions in c.6527insC and Δ G variants are shown in red. (B and C) Macroscopic appearance of human skin (delineated by dotted line) regenerated from clones 11 (B) and 40 (C). (D and E) Dermal-epidermal adhesion test. Detachment of epidermis (blue arrows) occurred after pulling from the edge of an incision on human skin grafts generated from clones 11 (D) and 40 (E). (F, G, H, and I) Immunofluorescence staining for the detection of human C7 (green) in grafts sections. In grafts from clones 11 (F) and 40 (G), C7 was retained within the cytoplasm of keratinocytes in the basal layer of epidermis. In contrast, grafts from normal human keratinocytes display C7 deposition in the BMZ (H). Grafts from unedited patient 2 keratinocytes were used as a negative control for staining (I). Cell nuclei were stained with DAPI (blue). Asterisks denote blisters formed between dermis and epidermis (F, G, and I). Scale bar, 50 μ m.

been developed for RDEB cells harboring a frameshift mutation in exon 80 of the *COL7A1* gene, highly prevalent in the Spanish and Latin American RDEB patient population,^{28,32} the same strategy

can be redeployed for mutations in other exons within *COL7A1* collagenous domain. In fact, *in vitro* translated C7 protein lacking the exon 105-encoded fragment conserved functionality in biochemical assays and promoted skin stability when injected in DEB mice.¹⁷ Likewise, RDEB patient keratinocytes transduced with retroviral vectors for expression of C7 variants lacking exons 73- and 80-encoded fragments secreted C7 homotrimers, and skin equivalents generated with these cells displayed restored C7 expression and dermal-epidermal adhesion.¹⁵ Although we have made use of previously established TALEN nucleases to facilitate locus-specific gene editing in our protocol, novel CRISPR/Cas9-based protocols will probably render remarkably increased editing efficiencies. This might permit working with polyclonal populations of corrected keratinocytes including gene-edited epidermal stem cells, which would be advantageous for the generation of clinically useful skin grafts. Still, monoclonal cellular therapy affords added benefits such as precise genotyping and biosafety characterization of individual clones^{24,26} prior to their use for generation of skin grafts, as shown here.

However, challenging the proliferative capabilities of individual epidermal stem cells to generate monoclonal grafts adds significant complexity to preclinical protocols. To circumvent this limitation, we have resorted to adding a small molecule inhibitor of Rho-associated kinase (Y-27632) to our keratinocyte cell culture medium, which greatly facilitates isolation and expansion of keratinocyte clones with stem cell features.³³ Although we are aware that the use of this reagent in clinical settings might raise some regulatory concerns, the keratinocyte stem cell clones isolated and characterized with our protocol did not display any sign of morphological transformation and rendered histologically normal skin grafts.

Under these conditions, we were able to isolate and expand over 100 clones, of which 8% showed expression of C7 variants, a proportion similar to that previously found with the immortalized cell line.¹¹ All clones selected for grafting (i.e., clones 11, 40 carrying a faulty *COL7A1* frame-restoring indel, and the biclonal population 19, carrying a *COL7A1* exon 80-deleted allele) showed engraftment and persistence *in vivo*. Moreover, upon subcloning to obtain a monoclonal population with an exon 80-deleted variant (i.e., Clone 19.C), long-term skin regeneration was also achieved. Although different C7 variants can be produced by NHEJ repair leading to *COL7A1* frame restoration, not all of them produce functional C7 protein. Skin grafts generated with keratinocytes carrying the 114-bp deletion allele that encoded an exon 80-lacking (Δ E80) variant displayed C7 deposition at the BMZ and dermal-epidermal adhesion. However, frame restoration by a smaller (1 bp) deletion that results in substitution of four amino acids within the exon 80-encoded sequence led to retention of the C7 protein in the basal layer of the epidermis and blister formation in the skin grafts. This suggests that only variants maintaining the Gly-X-Y pattern in the C7 triple helix-forming domain are appropriately processed and secreted by the keratinocytes and fit for anchoring fibril formation.

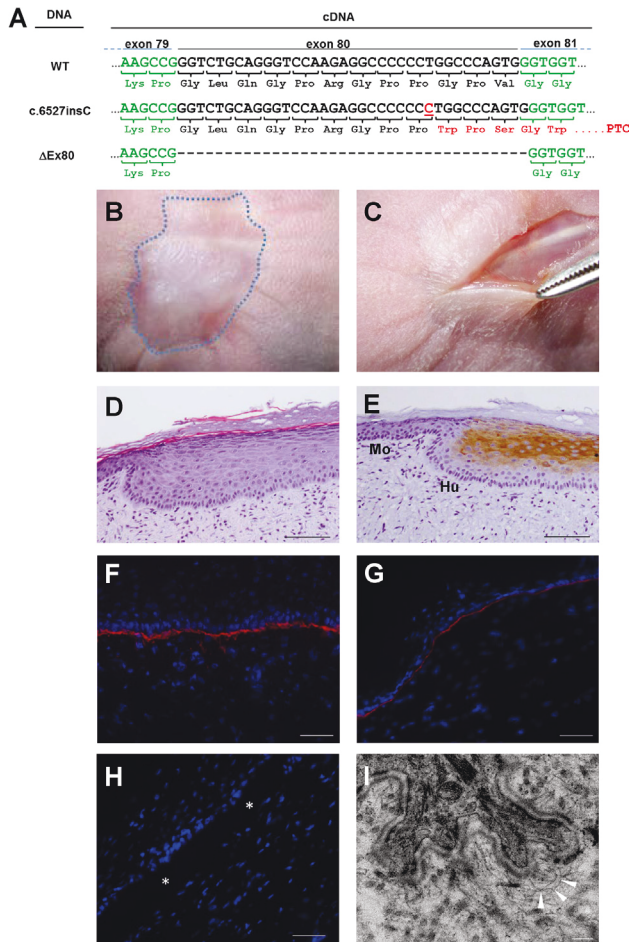


Figure 6. In Vivo Skin Regeneration from Frame-Restored Patient Keratinocyte Clone 19.C Expressing a C7 Variant Lacking the Exon 80-Encoded Sequence

(A) *COL7A1* cDNA and C7 amino acid sequences for WT, c.6527insC, and ΔE80 (114-bp deletion) alleles. Amino acid substitutions in c.6527insC are shown in red. (B) Macroscopic appearance of a representative human skin (delineated by dotted line) regenerated from clone 19.C. (C) Demonstration of dermal-epidermal adhesion in patient skin regenerated from clone 19.C. Firm pulling from the edge of an incision did not cause dermal-epidermal detachment. (D) H&E staining of regenerated patient skin showing epidermal-dermal adhesion and normal epidermal architecture. Scale bar, 100 μm. (E) Immunohistochemical staining using an antibody specific for human involucrin to show normal human epidermal differentiation of the gene-corrected patient skin graft at the mouse (Mo)-human (Hu) skin boundary. Scale bar, 100 μm. (F, G, and H) Immunofluorescence staining using an antibody specific for human C7 (red). Normal C7 deposition was found along the BMZ of a gene-corrected patient skin graft regenerated from clone 19.C keratinocytes (F) and in normal human keratinocyte positive control graft (G). No C7 staining was found in sections of a negative control graft regenerated from unedited patient 2 keratinocytes (H). Cell nuclei were stained with DAPI (blue). Asterisks denote blistering between dermis and epidermis. Scale bar, 50 μm. (I) Electron microscopy analysis showed the presence of mature anchoring fibrils (arrowheads) at the dermal-epidermal junction of gene-corrected patient skin regenerated from clone 19.C keratinocytes. Scale bar, 200 nm.

Our multiple grafting experiments provide proof of the clinical potential of clonal gene therapy protocols based on the excision of exons containing pathogenic mutations. Conceivably, improved gene editing tools will bring the combined genetic and cellular approach to a higher feasibility level.

MATERIALS AND METHODS

Culture of Primary RDEB Patient Keratinocytes and Transduction with Ad-TALENs T6/T7

Patient keratinocytes were originally obtained from skin biopsies of two RDEB (RDEB-sev gen) patients carrying the c.6527insC homozygous mutation in the *COL7A1* gene.^{28,34} Clinical features of these patients have been previously described (patients 4 and 9 in Escámez et al.²⁸). Skin biopsies were obtained from patients after approval from the Ethics Committee of the collaborating hospital upon informed consent. Primary human keratinocytes were cultured as previously described.²⁵ Human primary RDEB keratinocytes (from patients P1 and P2) were plated onto lethally irradiated 3T3-J2 cells and cultured in keratinocyte growth complete FAD (cFAD) medium, a DMEM, and Ham's F12 media mixture (3:1) containing fetal bovine serum (10%), penicillin-streptomycin (1%), glutamine (2%), insulin (5 μg/mL), adenine (0.18 mmol/L), hydrocortisone (0.4 μg/ml), cholera toxin (0.1 nmol/L), triiodothyronine (2 nmol/L), epidermal growth factor (EGF) (10 ng/mL), and Y-27632 ROCK inhibitor (Sigma) at 10 μM. For viral transduction, cells were trypsinized and infected in suspension with the TALEN-expressing adenoviral vectors (MOI, 300) in the presence of polybrene (8 μg/mL) (Sigma, St. Louis, MO). 1×10^6 transduced keratinocytes were then plated in a 35-mm dish without feeder layer in CnT-57 (CellnTec, Bern, Switzerland) medium and cultured at 37°C for 24 hr followed by 48 hr at 30°C. Cells were then trypsinized and plated at low density in 100-mm plates (10^3 cells/plate) with 2×10^6 lethally irradiated 3T3 feeder cells per plate, to obtain isolated clones. Cell clones were then collected using polystyrene cloning cylinders (Sigma, St. Louis, MO) and expanded for cryopreservation and genomic DNA extraction.

Cell I (Surveyor) Analysis

Genomic DNA was isolated by isopropanol precipitation of keratinocytes lysates (lysis buffer was Tris [pH 8], 100 mM, EDTA 5 mM, SDS 0.2%, NaCl 200 mM, 1 mg/mL proteinase K [Roche Diagnostics, Mannheim, Germany]) and resuspended in Tris/EDTA (TE) buffer. Approximately 100 ng of genomic DNA were used for PCR amplification. PCR fragments spanning the TALENs' target sites were generated with primers F1/R. F: 5'-gtgagtgtggctgaagcac-3'; R, 5'-accaccaaggaaactga-3'. PCR program TD 68-63 was as follows: 94°C for 3 min, five cycles of 94°C for 30 s, 68°C for 30 s, 72°C for 45 s, decreasing annealing temperature 1°C every cycle, followed by 30 cycles of 94°C for 30 s, 63°C for 30 s, 72°C for 45 s, then 72°C for 7 min. PCR products were subjected to melting and reannealing to yield heteroduplex DNA, digested with Surveyor nuclease (IDT, Iowa, IA) at 42°C for 1 hr, resolved in 1.5% agarose gels and visualized by ethidium bromide staining.

Genotyping for Detection of Indel Carrying Clones

Genomic DNA isolation and PCR amplification with primers F1/R were performed as described above. PCR products were treated with illustra ExoProStar (GE Healthcare, UK), sequenced using Big Dye Terminator V.1.1 Cycle Sequencing kit (Thermo Fisher, Waltham, MA), and examined on a 3730 DNA Analyzer (Life Technologies, Carlsbad, CA). Chromatograms were analyzed using Sequencher (Gene Codes, Ann Harbor, MI) and Chromas (Technelysium, Australia) software.

Off-Target Analysis

Potential off-target sites were predicted using the PROGNOS software to search the hg19 genome for the TALEN pair targeting the 5'-TGCCCTCTCTATGTAGGGT NN...NN AGGCCCCCCC TGGCCCA-3', using the following RVDs:

left, 01NN02HD03HD04HD05NG06HD07NG08HD09NG10NI11N G12NN13NG14NI15NN16NN17NN18NG; right, 01NN02NN03NN 04HD05HD06NI07NN08NN09NN10NN11NN12NN13NN14HD15 HD16NG, allowing up to six mismatches in each nuclease half-site and spacing distances between 10 to 28 bp. Homodimers and heterodimers of the nucleases were included in the prediction. Predicted off-target sites (Table S1) were PCR amplified using specific primer pairs (Table S2) and PCR products were analyzed using the Surveyor kit as described above.

COL7A1 Transcription Analysis by RT-PCR and Real-Time qPCR

Total RNA was extracted from keratinocytes with miRNeasy Mini Kit (QIAGEN, Hilden, Germany) and complementary DNA (cDNA) was synthesized using the SuperScript III First-Strand Synthesis System (Invitrogen, Carlsbad, CA). The following primers were used to amplify 241 (unedited) and 205 (exon 80 deleted) bp fragments spanning exons 78–84 of *COL7A1*: F, 5'-AGGGGTCAGGACGGCAAC-3' and R, 5'-CAGCTCCAGTAGGTCCAGTCAG-3'. The PCR program was as follows: 94°C for 3 min, five cycles of 94°C for 30 s, 68°C for 30 s, 72°C for 45 s, decreasing annealing temperature 1°C every cycle, followed by 25 cycles of 94°C for 30 s, 63°C for 30 s, 72°C for 45 s, then 72°C for 7 min. The human glyceraldehyde-3-phosphate dehydrogenase gene (*GAPDH*) was analyzed as a loading control with *GAPDH*-specific primers: F, 5'-accacagtcctgcatcac-3', and R, 5'-tcaccacccctgtgctgt-3'. For the real-time qPCR analysis, 1:20 dilutions of each cDNA synthesis reaction were analyzed in triplicate using Taqman gene-expression assays Hs00164310_m1 (*COL7A1* exon64 probe), Hs01574801_g1 (*COL7A1* exon80 probe), and Hs02758991_g1 (*GAPDH* probe, control). Amplification was performed using a QuantStudio 6 Flex Real-Time PCR System (Applied Biosystems).

Western Blot Analysis

Keratinocytes were lysed in protein extraction buffer (50 mM Tris-HCl [pH 7.5], 100 mM NaCl, 1% Nonidet P-40, 4 mM EDTA) containing proteinase inhibitors cocktail (Complete Mini, EDTA-free; Roche Diagnostics, Mannheim, Germany). Lysates were incubated for 30 min on ice and centrifuged at 15,000 × g for

30 min at 4°C. Supernatants were collected and protein concentrations were measured using the Bradford assay (BioRad, Hercules, CA). For each sample, 40 µg of total protein was resolved on NuPAGE Novex 3%–8% Tris-Acetate gel electrophoresis (Invitrogen, Carlsbad, CA) and electrotransferred to nitrocellulose membranes (Invitrogen, Carlsbad, CA). For type VII collagen analysis, blots were probed with a monospecific polyclonal anti C7 antibody (a generous gift from Dr A. Nystrom). Antibodies against vinculin (Abcam) or α -tubulin (Sigma, St. Louis, MO) were used as loading controls. Visualization was performed by incubating with HRP-conjugated anti-rabbit antibody (Amersham, Burlington, MA) and West Pico Chemiluminescent Substrate (Pierce, Rockford, IL).

Immunofluorescence and Immunohistochemical Staining

For immunofluorescence detection of C7 in keratinocytes or in skin graft sections, cells grown on glass coverslips or 7-µm frozen sections of grafted skin tissue were fixed in methanol/acetone (1:1) for 10 min at –20°C. After washing three times in PBS and once in PBS with 3% BSA (Sigma Aldrich, St. Louis, MO) for 30 min, cells or cryosections were incubated with monospecific polyclonal anti C7 antibody (a generous gift from Dr A. Nystrom) at 1:5,000 dilution. Secondary antibody (Alexa Fluor 488, Invitrogen, Carlsbad, CA) was used at 1:1,000 dilution. After the final washing step in PBS, preparations were mounted using Mowiol (Hoechst, Somerville, NJ) mounting medium and DAPI 20 µg/m (Sigma) for nuclei visualization. H&E staining was performed on paraffin-embedded skin samples. Immunoperoxidase staining for human involucrin was performed using rabbit SY5 monoclonal antibody (Sigma) using the ABC peroxidase kit (Vector) with diaminobenzidine as a substrate.

Generation of Skin Equivalents and Grafting onto Immunodeficient Mice

Keratinocytes were seeded on RDEB-containing fibrin dermal equivalents prepared as previously described.³⁵ Bioengineered skin equivalents were grafted onto the back of immunodeficient nu/nu mice.²⁵ Twelve weeks after grafting, mice were sacrificed and grafts harvested for skin immunofluorescence, immunohistochemical and histological analysis, and electron microscopy studies. Animal studies were approved by our institutional animal care and use committee according to all legal regulations.

Electron Microscopy

Specimens of ca. 0.4 × 0.3 cm were fixed for at least 2 hr at room temperature in 3% glutaraldehyde solution in 0.1 M cacodylate buffer (pH 7.4), cut into pieces of ca. 1 mm³, washed in buffer, postfixed for 1 hr at 4°C in 1% osmium tetroxide, rinsed in water, dehydrated through graded ethanol solutions, transferred into propylene oxide, and embedded in epoxy resin (glycidether 100). Semithin and ultrathin sections were cut with an ultramicrotome (Reichert Ultracut E). Ultrathin sections were treated with uranyl acetate and lead citrate and examined with an electron microscope (JEM 1400) equipped with a 2k CCD camera (TVIPS).

SUPPLEMENTAL INFORMATION

Supplemental Information includes five figures and two tables and can be found with this article online at <https://doi.org/10.1016/j.omtn.2018.01.009>.

AUTHOR CONTRIBUTIONS

R.M., A.M., and F.L. designed the experiments. R.M., A.M., C.C., and J.B. performed molecular and cellular studies. S.G.L., M.J.E., and M.D.R. provided reagents and ethical approval for the studies. A.H., B.D., and N.I. performed animal experiments and histological analysis. I.H. performed the electron microscopy analysis. A.M., F.L., and R.M. wrote the paper.

CONFLICTS OF INTEREST

All authors declare no conflict of interest.

ACKNOWLEDGMENTS

The study was mainly supported by DEBRA International—funded by DEBRA Austria (grant termed as Larcher 1). Additional funds come from Spanish grants SAF2013-43475-R and SAF2017-86810-R from the Ministry of Economy and Competitiveness and PI14/00931 and PI17/01747 from the Instituto de Salud Carlos III, all of them co-funded with European Regional Development Funds (ERDF). Authors are indebted to Jesus Martínez and Edilia De Almeida for animal maintenance and care.

REFERENCES

1. Fine, J.D., Bruckner-Tuderman, L., Eady, R.A., Bauer, E.A., Bauer, J.W., Has, C., Heagerty, A., Hintner, H., Hovnanian, A., Jonkman, M.F., et al. (2014). Inherited epidermolysis bullosa: updated recommendations on diagnosis and classification. *J. Am. Acad. Dermatol.* *70*, 1103–1126.
2. Mavilio, F., Pellegrini, G., Ferrari, S., Di Nunzio, F., Di Iorio, E., Recchia, A., Maruggi, G., Ferrari, G., Provasi, E., Bonini, C., et al. (2006). Correction of junctional epidermolysis bullosa by transplantation of genetically modified epidermal stem cells. *Nat. Med.* *12*, 1397–1402.
3. Bauer, J.W., Koller, J., Muraier, E.M., De Rosa, L., Enzo, E., Carulli, S., Bondanza, S., Recchia, A., Muss, W., Diem, A., et al. (2017). Closure of a large chronic wound through transplantation of gene-corrected epidermal stem cells. *J. Invest. Dermatol.* *137*, 778–781.
4. Sipsashvili, Z., Nguyen, N.T., Gorell, E.S., Loutit, K., Khuu, P., Furukawa, L.K., Lorenz, H.P., Leung, T.H., Keene, D.R., Rieger, K.E., et al. (2016). Safety and wound outcomes following genetically corrected autologous epidermal grafts in patients with recessive dystrophic epidermolysis bullosa. *JAMA* *316*, 1808–1817.
5. Hirsch, T., Rothoefl, T., Teig, N., Bauer, J.W., Pellegrini, G., De Rosa, L., Scaglione, D., Reichelt, J., Klausegger, A., Kneisz, D., et al. (2017). Regeneration of the entire human epidermis using transgenic stem cells. *Nature* *551*, 327–332.
6. Hennig, K., Raasch, L., Kolbe, C., Weidner, S., Leisegang, M., Uckert, W., Titeux, M., Hovnanian, A., Kuehlcke, K., and Loew, R. (2014). HEK293-based production platform for γ -retroviral (self-inactivating) vectors: application for safe and efficient transfer of COL7A1 cDNA. *Hum. Gene Ther. Clin. Dev.* *25*, 218–228.
7. Osborn, M.J., Starker, C.G., McElroy, A.N., Webber, B.R., Riddle, M.J., Xia, L., DeFeo, A.P., Gabriel, R., Schmidt, M., von Kalle, C., et al. (2013). TALEN-based gene correction for epidermolysis bullosa. *Mol. Ther.* *21*, 1151–1159.
8. Webber, B.R., Osborn, M.J., McElroy, A.N., Twaroski, K., Lonetree, C.L., DeFeo, A.P., Xia, L., Eide, C., Lees, C.J., McElmurry, R.T., et al. (2016). CRISPR/Cas9-based genetic correction for recessive dystrophic epidermolysis bullosa. *NPJ Regen. Med.* *1*, 16014.
9. Shinkuma, S., Guo, Z., and Christiano, A.M. (2016). Site-specific genome editing for correction of induced pluripotent stem cells derived from dominant dystrophic epidermolysis bullosa. *Proc. Natl. Acad. Sci. USA* *113*, 5676–5681.
10. Izmiryan, A., Danos, O., and Hovnanian, A. (2016). Meganuclease-mediated COL7A1 gene correction for recessive dystrophic epidermolysis bullosa. *J. Invest. Dermatol.* *136*, 872–875.
11. Chamorro, C., Mencía, A., Almarza, D., Duarte, B., Büning, H., Sallach, J., Hausser, I., Del Río, M., Larcher, F., and Murillas, R. (2016). Gene editing for the efficient correction of a recurrent COL7A1 mutation in recessive dystrophic epidermolysis bullosa keratinocytes. *Mol. Ther. Nucleic Acids* *5*, e307.
12. Hainzl, S., Peking, P., Kocher, T., Muraier, E.M., Larcher, F., Del Rio, M., Duarte, B., Steiner, M., Klausegger, A., Bauer, J.W., et al. (2017). COL7A1 editing via CRISPR/Cas9 in recessive dystrophic epidermolysis bullosa. *Mol. Ther.* *25*, 2573–2584.
13. Niks, E.H., and Aartsma-Rus, A. (2017). Exon skipping: a first in class strategy for Duchenne muscular dystrophy. *Expert Opin. Biol. Ther.* *17*, 225–236.
14. Turczynski, S., Titeux, M., Pironon, N., and Hovnanian, A. (2012). Antisense-mediated exon skipping to reframe transcripts. *Methods Mol. Biol.* *867*, 221–238.
15. Turczynski, S., Titeux, M., Tonasso, L., Décha, A., Ishida-Yamamoto, A., and Hovnanian, A. (2016). Targeted exon skipping restores type VII collagen expression and anchoring fibril formation in an in vivo RDEB model. *J. Invest. Dermatol.* *136*, 2387–2395.
16. Bremer, J., Bornert, O., Nyström, A., Gostynski, A., Jonkman, M.F., Aartsma-Rus, A., van den Akker, P.C., and Pasmooij, A.M. (2016). Antisense oligonucleotide-mediated exon skipping as a systemic therapeutic approach for recessive dystrophic epidermolysis bullosa. *Mol. Ther. Nucleic Acids* *5*, e379.
17. Bornert, O., Kühl, T., Bremer, J., van den Akker, P.C., Pasmooij, A.M., and Nyström, A. (2016). Analysis of the functional consequences of targeted exon deletion in COL7A1 reveals prospects for dystrophic epidermolysis bullosa therapy. *Mol. Ther.* *24*, 1302–1311.
18. Ousterout, D.G., Kabadi, A.M., Thakore, P.I., Perez-Pinera, P., Brown, M.T., Majoros, W.H., Reddy, T.E., and Gersbach, C.A. (2015). Correction of dystrophin expression in cells from Duchenne muscular dystrophy patients through genomic excision of exon 51 by zinc finger nucleases. *Mol. Ther.* *23*, 523–532.
19. Ousterout, D.G., Perez-Pinera, P., Thakore, P.I., Kabadi, A.M., Brown, M.T., Qin, X., Fedrigo, O., Mouly, V., Tremblay, J.P., and Gersbach, C.A. (2013). Reading frame correction by targeted genome editing restores dystrophin expression in cells from Duchenne muscular dystrophy patients. *Mol. Ther.* *21*, 1718–1726.
20. Long, C., Amoasii, L., Mireault, A.A., McAnally, J.R., Li, H., Sanchez-Ortiz, E., Bhattacharyya, S., Shelton, J.M., Bassel-Duby, R., and Olson, E.N. (2016). Postnatal genome editing partially restores dystrophin expression in a mouse model of muscular dystrophy. *Science* *351*, 400–403.
21. Nelson, C.E., Hakim, C.H., Ousterout, D.G., Thakore, P.I., Moreb, E.A., Castellanos Rivera, R.M., Madhavan, S., Pan, X., Ran, F.A., Yan, W.X., et al. (2016). In vivo genome editing improves muscle function in a mouse model of Duchenne muscular dystrophy. *Science* *351*, 403–407.
22. Tabebordbar, M., Zhu, K., Cheng, J.K.W., Chew, W.L., Widrick, J.J., Yan, W.X., Maesner, C., Wu, E.Y., Xiao, R., Ran, F.A., et al. (2016). In vivo gene editing in dystrophic mouse muscle and muscle stem cells. *Science* *351*, 407–411.
23. Wu, W., Lu, Z., Li, F., Wang, W., Qian, N., Duan, J., Zhang, Y., Wang, F., and Chen, T. (2017). Efficient in vivo gene editing using ribonucleoproteins in skin stem cells of recessive dystrophic epidermolysis bullosa mouse model. *Proc. Natl. Acad. Sci. USA* *114*, 1660–1665.
24. Droz-Georget Lathion, S., Rochat, A., Knott, G., Recchia, A., Martinet, D., Benmohammed, S., Grasset, N., Zaffalon, A., Besuchet Schmutz, N., Savioz-Dayer, E., et al. (2015). A single epidermal stem cell strategy for safe ex vivo gene therapy. *EMBO Mol. Med.* *7*, 380–393.
25. Duarte, B., Miselli, F., Murillas, R., Espinosa-Hevia, L., Cigudosa, J.C., Recchia, A., Del Rio, M., and Larcher, F. (2014). Long-term skin regeneration from a gene-targeted human epidermal stem cell clone. *Mol. Ther.* *22*, 1878–1880.
26. Larcher, F., Dellambra, E., Rico, L., Bondanza, S., Murillas, R., Cattoglio, C., Mavilio, F., Jorcano, J.L., Zambruno, G., and Del Rio, M. (2007). Long-term engraftment of single genetically modified human epidermal holoclones enables safety pre-assessment of cutaneous gene therapy. *Mol. Ther.* *15*, 1670–1676.

27. Hovnanian, A., Rochat, A., Bodemer, C., Petit, E., Rivers, C.A., Prost, C., Fraitag, S., Christiano, A.M., Uitto, J., Lathrop, M., et al. (1997). Characterization of 18 new mutations in COL7A1 in recessive dystrophic epidermolysis bullosa provides evidence for distinct molecular mechanisms underlying defective anchoring fibril formation. *Am. J. Hum. Genet.* 61, 599–610.
28. Escámez, M.J., García, M., Cuadrado-Corrales, N., Llames, S.G., Charlesworth, A., De Luca, N., Illera, N., Sánchez-Jimeno, C., Holguín, A., Duarte, B., et al. (2010). The first COL7A1 mutation survey in a large Spanish dystrophic epidermolysis bullosa cohort: c.6527insC disclosed as an unusually recurrent mutation. *Br. J. Dermatol.* 163, 155–161.
29. Anglani, F., Picci, L., Camporese, C., and Zacchello, F. (1990). Heteroduplex formation in polymerase chain reaction. *Am. J. Hum. Genet.* 47, 169–170.
30. Ousterout, D.G., Kabadi, A.M., Thakore, P.I., Majoros, W.H., Reddy, T.E., and Gersbach, C.A. (2015). Multiplex CRISPR/Cas9-based genome editing for correction of dystrophin mutations that cause Duchenne muscular dystrophy. *Nat. Commun.* 6, 6244.
31. Fine, E.J., Cradick, T.J., Zhao, C.L., Lin, Y., and Bao, G. (2014). An online bioinformatics tool predicts zinc finger and TALE nuclease off-target cleavage. *Nucleic Acids Res.* 42, e42.
32. Rodríguez, F.A., Gana, M.J., Yubero, M.J., Zillmann, G., Krämer, S.M., Catalán, J., Rubio-Astudillo, J., González, S., Liu, L., Ozoemena, L., et al. (2012). Novel and recurrent COL7A1 mutations in Chilean patients with dystrophic epidermolysis bullosa. *J. Dermatol. Sci.* 65, 149–152.
33. Chapman, S., McDermott, D.H., Shen, K., Jang, M.K., and McBride, A.A. (2014). The effect of Rho kinase inhibition on long-term keratinocyte proliferation is rapid and conditional. *Stem Cell Res. Ther.* 5, 60.
34. Chamorro, C., Almarza, D., Duarte, B., Llames, S.G., Murillas, R., García, M., Cigudosa, J.C., Espinosa-Hevia, L., Escámez, M.J., Mencía, A., et al. (2013). Keratinocyte cell lines derived from severe generalized recessive epidermolysis bullosa patients carrying a highly recurrent COL7A1 homozygous mutation: models to assess cell and gene therapies in vitro and in vivo. *Exp. Dermatol.* 22, 601–603.
35. Llames, S.G., Del Rio, M., Larcher, F., García, E., García, M., Escamez, M.J., Jorcano, J.L., Holguín, P., and Meana, A. (2004). Human plasma as a dermal scaffold for the generation of a completely autologous bioengineered skin. *Transplantation* 77, 350–355.

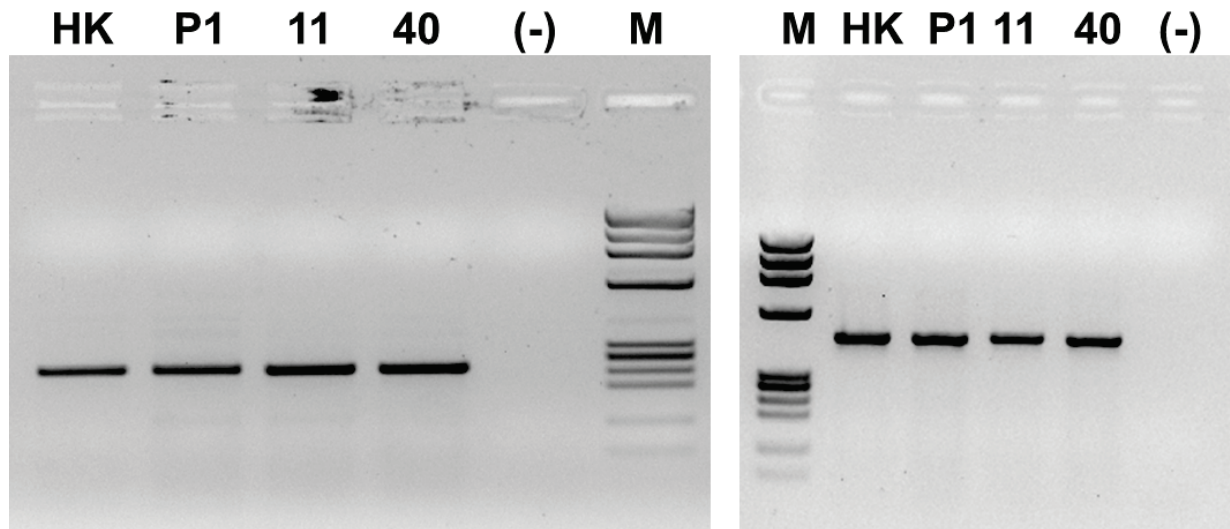
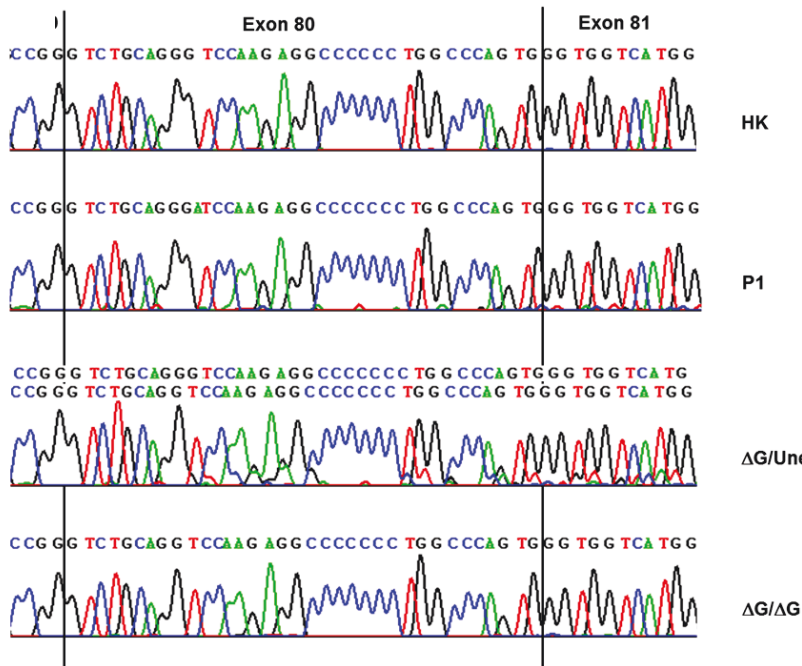
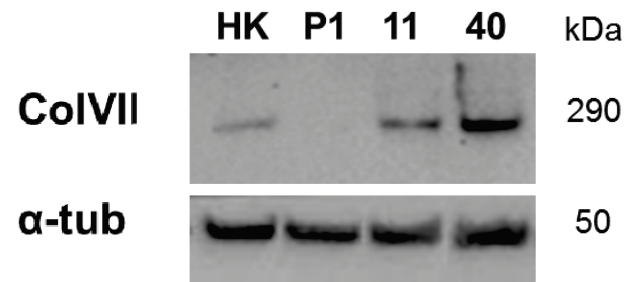
Supplemental Information

Deletion of a Pathogenic Mutation-Containing

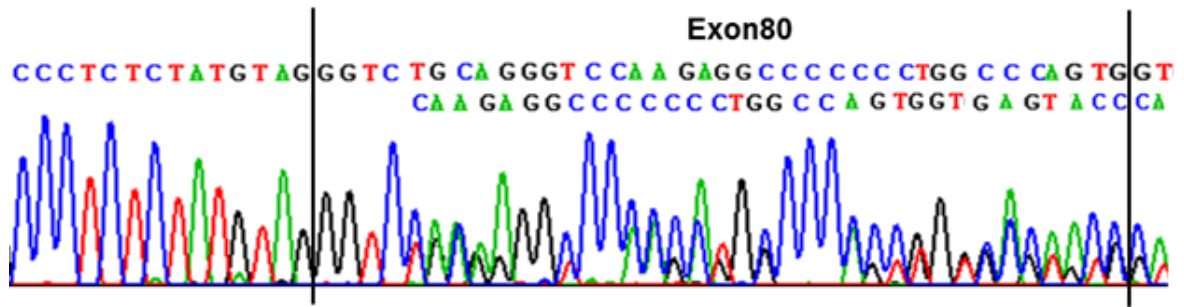
Exon of *COL7A1* Allows Clonal Gene Editing

Correction of RDEB Patient Epidermal Stem Cells

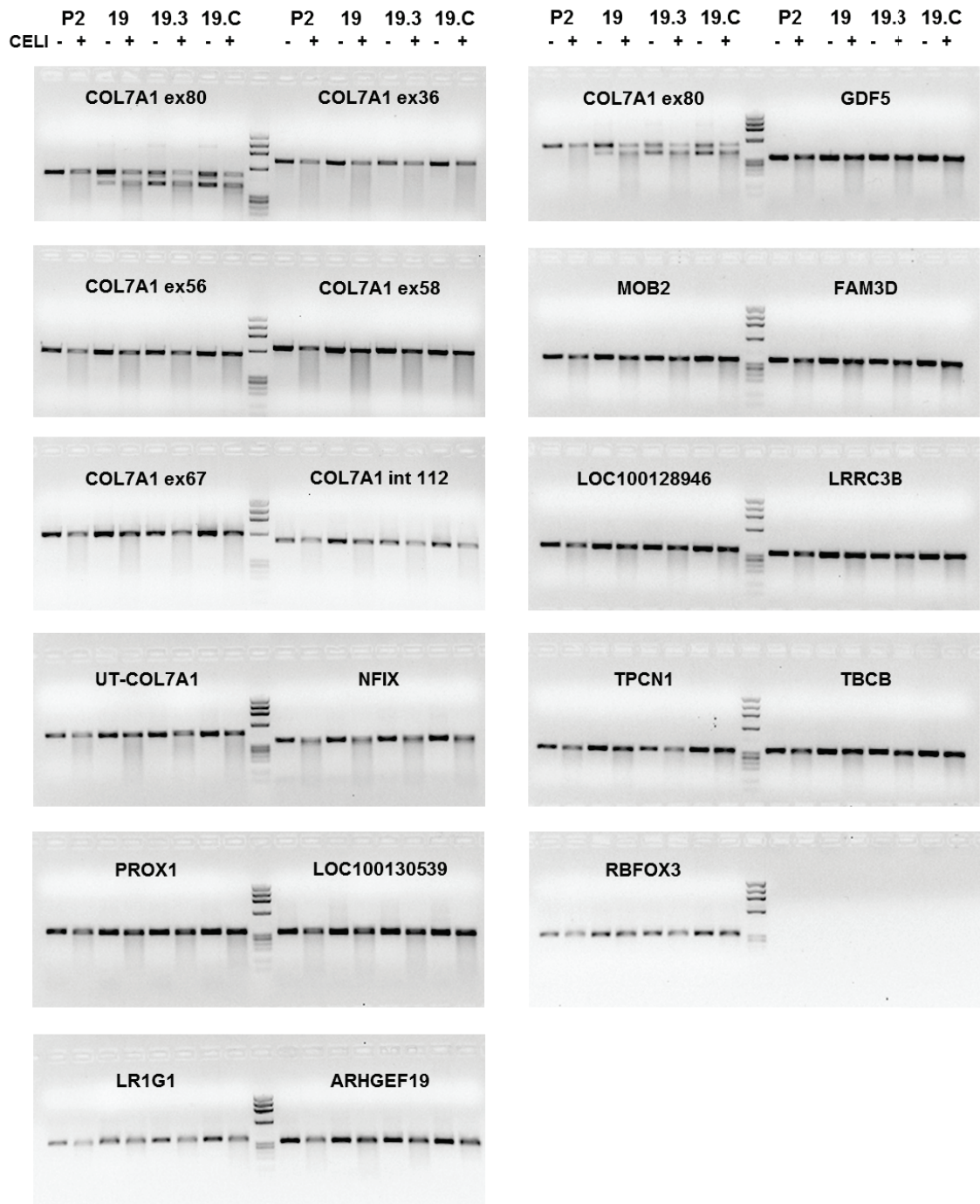
Ángeles Mencía, Cristina Chamorro, Jose Bonafont, Blanca Duarte, Almudena Holguin, Nuria Illera, Sara G. Llames, Maria José Escámez, Ingrid Hausser, Marcela Del Río, Fernando Larcher, and Rodolfo Murillas

A**B****C**

Supplementary Figure S1. *COL7A1* gene expression in frame-restored P1 keratinocytes clones 11 and 40, containing a 1 bp ΔG deletion in one (clone 11) or both (clone 40) *COL7A1* alleles. (A) left panel, RT-PCR analysis of *COL7A1* expression from healthy human control (HK), P1 patient (P1), clone 11 and clone 40 keratinocyte RNA samples. (-), negative control without cDNA; M is IX molecular weight marker. Right panel, RT-PCR analysis of GAPDH expression, as a loading control. (B) Sequencing chromatograms for RT-PCR products. Frame-restored transcripts were found for the ΔG mutation-carrying clones 11 (monoallelically modified, overlapping chromatograms) and 40 (biallelically modified). (C) Western blot detection of C7 (ColVII) in *COL7A1* frame restored clones 11 and 40. Note increased amounts of C7 in these clones, compared to normal human keratinocytes (HK). No expression was found in unedited P1 patient keratinocytes (P1). α -tubulin expression was used as a loading control (lower panel).



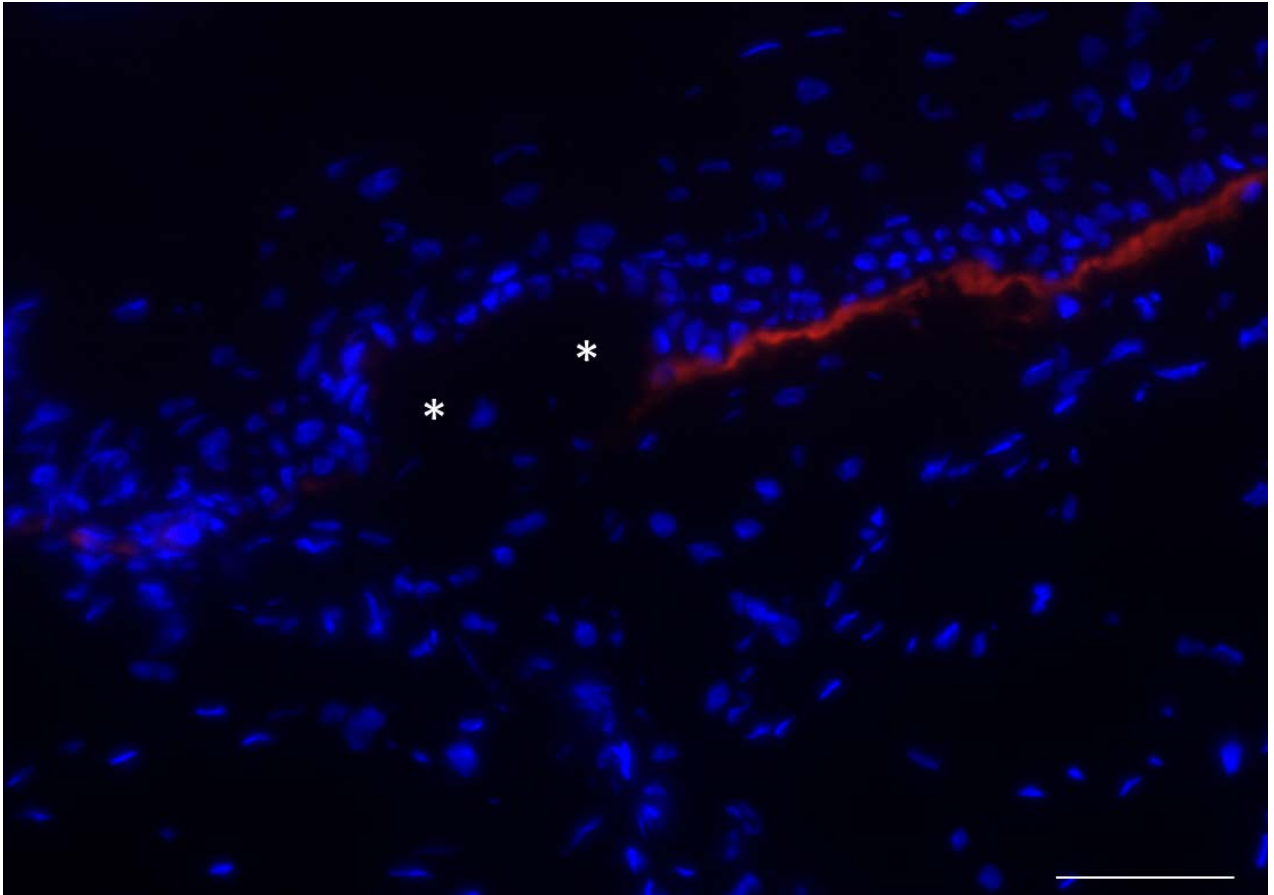
Supplementary Figure S2. Clone 19n genotype. Sanger sequencing chromatogram of C7-negative clone 19n revealed the presence of overlapping chromatograms for the c.6527insC (unmodified, upper nucleotide sequence) and c.6503_6511del9 (9 bp deletion, lower nucleotide sequence) alleles.



Supplementary Figure S3. PROGNOS-predicted off-target sites (Supplementary Table 1) for TALENs T6/T7 homo and heterodimers were PCR amplified using genomic DNA from keratinocyte clones 19, 19.3, 19.C and patient 2 (P2) keratinocytes, using specific primer pairs (Supplementary Table 2). PCR products were then screened for indels using the Surveyor (Cell) assay. COL7A1 exon 80 on-target site was included as a positive control for indel generation by T6/T7 TALENs (left side, upper panels).



Supplementary Figure S4. Histological (H&E staining) analysis of a human skin graft regenerated from clone 11, expressing a C7 variant with a 4 aminoacids substitution. Consistent with the inability to promote epidermal-dermal attachment by this C7 variant, the epidermis separated from the dermis (not seen in the picture) during sample processing. Otherwise, basal cells of the epidermis and epidermal differentiation appear normal, suggesting that intracellular accumulation of C7 is not cytotoxic. Scale bar: 100 μ m



Supplementary Figure S5. Immunofluorescence detection of C7 (red) on a section of a skin graft generated with mixed clone 19 keratinocytes. C7 deposition along the BMZ coincided with areas showing dermal-epidermal attachment. Blistering spots (asterisks) matched areas negative for C7, likely originating from uncorrected epidermal stem cells. Cell nuclei were stained with DAPI (blue). Scale bar: 50 μ m.

Supplementary Table 1. Potential off target sites predicted by PROGNOS software. Nucleotides mismatching TALENs-binding consensus sequences are shown in red.

chromosome	gene	genomic region	Match type	target sequence F	target sequence R	number of mismatches
Chr3	COL7A1	exon 80	L14R	TGCCCTCTCTATGTAGGGT	TGGGCCAGGGGGGCCT	0
Chr3	COL7A1	exon 36	R10R	TGGaCCA ct GGGGa Cc	gaa GCC ct GGGGG CCa	11
Chr3	COL7A1	exon 56	R25R	ggg aCC t GaGGG ct CC T	ggg tCC t GGGG gac CC T	12
Chr3	COL7A1	exon 58	R17R	TG cca CAGGGaGaGCCT	TGGGCC ctc GaGGa CCc	11
Chr3	COL7A1	exon 67	R19R	Tt Gga C cccaGGGGCCT	ct GGCCAGGaGGG c CCa	11
Chr3	COL7A1	intron 112	R21R	TGGGCC t GGGaGGGCCT	TGa Ggg AGG t aGGGCC c	8
Chr3	COL7A1	intron 112	R10R	a GGGCC t GGG t GGGCCT	TGa Ggg AGG t aGGGCC c	9
Chr3	UT-COL7A1	5'-UTR	R27R	TG ct CCAGG t GGGG ggc	AGGC ag CC ct t cCC cc	11
Chr19	NFIX	intron	R22R	c GG t ggAGG c GGGGCCT	TGGGCC c GGGGGGGCCT	6
Chr1	PROX1	intron	R17R	ca GG g AGGGaGGCCT	TGGGCC a tGGGaGGCCT	7
Chr10	LOC100130539	intergenic	R24R	Ta G c CaAGGG aa G c CC T	TGGGCCAG aa GG ca CC T	10
Chr3	LRIG1	intron	R16R	TGGGCC c GGGGaGGCCT	TGGG ga AGGGG Ga G c CC c	7
Chr1	ARHGEF19	intron	R12R	TGGG c agGG ca GGGGCT	gg G t CCAGGGGGGCCT	7
Chr20	GDF5	exon	R17R	ca GGCCAGG att GGCCa	c GGGCCAGGGGGGCCT	7
Chr11	MOB2	intron	R24R	TGGGCCAGGGGG c CC T	ct GGCCAG tc GGG a CCa	7
Chr3	FAMD3	intron	R28R	Ta G a CCAGGGaGGGCC c	TGGGCCAGG ctaca CC T	9
Chr22	LOC100128946	intergenic	R13R	ca G c CCAGGGG a GCCT	TGGGCC c GGGG aa GCCT	7
Chr3	LRRC3B	intergenic	R17R	TGGGCCAGGGaGaGCCT	TG ac Ca t GGGaGGGCC c	8
Chr12	TPCN1	intron	R11R	TGGG g CAGGaGGGCCT	TGGG ag AGGaGGaGCCT	6
Chr19	TBCB	intron	R20R	TG a G C tAGGaGGG c CC T	T caGCCAGaGGG a GCCT	8
Chr17	RBFOX3	intron	R23R	TGG a CCAGGG c ctGCCT	TG c GCCAG aa gAGGCCT	8

Supplementary Table 2. List of primers used for PCR amplification of potential off-target sites.

Gene	Forward primer	Reverse primer	Length (bp)
<i>COL7A1 ex80</i>	GTGAGTGGTGGCTGAAGCAC	ACCCACCAAGGAACTGA	494
<i>COL7A1ex34-36</i>	CCCAGGGTTCTTCCACAGG	CATGGTGAGGATGGGGGTAA	693
<i>COL7A1ex54-56</i>	GGAGGCATGGGGTGATGG	CCCAAGTCCCCGAAGCA	643
<i>COL7A1ex56-60</i>	GATCCCTGGAGCCCCTC	CACCCTGTGGAAAATAGAGTGGTAA	633
<i>COL7A1ex65-67</i>	CACAGGCCATGCTCCAAGA	GGCAGAACACAAGGGGTCA	603
<i>COL7A1EX111-112</i>	AGCTCTGACTCCTGATCCCT	GGGACTATGGTGAGACTGCA	508
<i>UT-COL7A1</i>	GCTGGAGGCAGTGAAGACCA	TCCCAGCACCCCTTTGAGAGA	452
<i>NFIX</i>	CTAGGCTTGAGTGTCTGATGTGTG	CAACTCCAATGGGGGAAGCC	357
<i>PROX1</i>	AGATGGGTGCAAACCTCACCTTC	ATTTGGGCACAGGCGTCTGG	331
<i>LOC100130539</i>	CTGTCTCGATTGCGATCCAGG	TGTTAGACAATGGGTGCAGCC	325
<i>LRIG1</i>	TTCCAGGGAATGGGGAAAGTG	GGGAAAACAGTGGTTATCAGCATGCATAG	357
<i>ARHGEF19</i>	GAGTTCCTCTGTCTCTTCATGG	ATTGTGCTGATCCACCTTCCAGA	326
<i>GDF5</i>	CTGTGTCAGGCCTCCTGTCT	CCAAACCAGAGGCACCTTTGCT	330
<i>MOB2</i>	AGAAGTGACCACTGGCAGGG	CTGGAAGCCACCTAGCAAGC	345
<i>FAM3D</i>	CTTTGGAGCAAAGCTGCAGGC	GAAGGGGCACCTTTACCTACTC	343
<i>LOC100128946</i>	CTCCCTGAGCGGGTGCTTTT	TGATGACGATGGCAGGGGCT	344
<i>LRR3B</i>	CTCATCTCTGCAGCTATCTGCTC	TGCTCCCATCTCCAAGCAGG	326
<i>TPCN1</i>	AGGGGAGAGCTGTTTTGGGC	AATCAAAGAGAACACGTGGCCGG	326
<i>TBCB</i>	AGACACCTCAGGGTGTCTCTTG	CAGCCTCCCAATGTACTGGGT	325
<i>RBFOX3</i>	AGTTCACCAGCCCTACGCAG	GCTTTGGGCTTTGCCAAGGG	327